SSRG International Journal of Electrical and Electronics Engineering
ISSN: 2348-8379/ https://doi.org/10.14445/23488379/IJEEE-V13I7P105

Volume 13 Issue 7, 91-112, July 2026

Original Article

Physics-Informed Hybrid Marine Predator and Harris Hawks Optimization for Deep-Sea Black Box Localization Using Passive Sonar Modeling

Afsar Ali[1], Kaja Mohideen[2], Vedachalam[3]

[1,2]*Department of ECE, B.S. Abdur Rahman Crescent Institute of Science and Technology, Tamil Nadu, India*
[3]*Deep Sea Technology, National Institute of Ocean Technology (NIOT), Tamil Nadu, India*

[2]*Corresponding Author : kajamohideen@crescent.education*

Received: 21 February 2026 Revised: 11 March 2026 Accepted: 19 June 2026 Published: 27 July 2026

Abstract - *Locating Underwater Locator Beacons (ULBs) in deep-sea conditions is still a significant challenge due to the severe Attenuation (acoustic) and complex multipath transmission, and the presence of high ambient ocean noise. Current localization methods tend to be based on simplified acoustic propagation models or computationally intensive physics-based solvers, thus limiting the accuracy of localization and the ability to deploy it in real-time in practical Search and Rescue (SAR) missions. In a bid to overcome these shortcomings, this paper suggests a physics-informed hybrid optimization framework of localizing black boxes in the deep sea through a combination of passive sonar modeling and a hybrid Marine Predator Algorithm-Harris Hawks Optimization (MPA-HHO) strategy. The proposed structure uses the standard passive sonar equation and realistic transmission loss models that consider the effects of spherical spreading, frequency-dependent absorption (approximately 6.57 dB/km at 37.5 kHz), and major deep-water propagation processes such as surface reflection, surface ducting, bottom bouncing, convergence zone propagation, deep sound channel effects, and dependable acoustic paths. The proposed hybrid model is in contrast to traditional standalone optimization models that typically do not incorporate the global exploration properties of MPA or the effective local exploitation properties of HHO to enhance localization accuracy and convergence behavior. The results of the simulation under the realistic conditions of a deep-ocean environment show that the proposed structure reaches a high level of fitness of 10.1 dB and that it converges in almost 45 iterations. The distance error is minimized to 0.03 km with a probability of detection of 0.98 in a 3 km range. Moreover, the framework reduces the search area of 10,000 km² to about 3.14 km2, which corresponds to over 99.9% search-space reduction, and only requires 11.8 seconds of execution time, a nearly 87% reduction in computational complexity compared to traditional ray-tracing techniques. The findings prove that the incorporation of realistic ocean acoustic physics with adaptable hybrid bio-inspired optimization has offered a robust, computationally efficient and reliable solution to deep-sea underwater locator beacon detection and near real-time SAR operations.*

Keywords - *Underwater Locator Beacon, Passive Sonar, Deep-Sea Acoustics, Transmission Loss Modeling, Multipath Propagation, Marine Predator Algorithm, Harris Hawks Optimization, Hybrid Metaheuristic Optimization, Search And Rescue.*

1. Introduction

The post-oceanic aviation accidents retrieval of aircraft black boxes has been one of the most difficult elements of maritime Search and Rescue (SAR) operations. In modern aircraft, Underwater Locator Beacons (ULBs) are installed that emit acoustic pulses at a standard frequency of 37.5 kHz with a source level of about 160-165 dB re 1 µPa at 1 m. Though these beacons are designed to facilitate the recovery operations up to almost 30 days, the accurate localization in a deep-sea environment remains challenging due to extreme acoustic attenuation, variability of ocean noise and the multipath propagation conditions [1, 2]. Effective retrieval of black boxes is very crucial to accident investigation, safety analysis, as well as prevention of future aviation calamities.

The historical cases of deep-sea aviation accidents have shown that black box recovery operations might take several weeks or months to accomplish, especially when search areas are hundreds or thousands of square kilometers [3, 4]. Even with highly sensitive hydrophones, the practical range of ULB signals is often less than 2500 m in depth in deep-sea environments, or less than 2500 m in depth offshore in the ocean. It has been previously reported that delayed or unsuccessful recoveries are often due to poor acoustic detectability of the beacon due to transmission loss and environmental variability rather than failure of the beacon [5, 6]. This has led to an increased research interest in current SAR applications in enhancing the localization capability of passive underwater acoustic systems.

Geometric spreading, absorption loss and environmental fluctuations are all key factors that influence underwater acoustic propagation in deep-sea environments. Absorption coefficients within the ULB frequency range of 37.5 kHz, at 37.5 kHz and conditions of water temperature, salinity, pH, and depth typically vary between 5 and 8 dB/km. The strength of the received signal can approach and even exceed the ambient ocean noise level, which is typically found between 55 and 65 dB re 1 µPa in deep-ocean regions with low surface activity [7, 8]. All of these conditions significantly reduce the Signal-To-Noise Ratio (SNR), hence the probability of detection and localization accuracy.

In addition to the attenuation effects, multipath effects are serious in acoustic propagation in deep water. Propagation of the acoustic energy can occur through a number of mechanisms such as direct paths, surface reflections, surface ducting, bottom bounce propagation, Convergence Zones (CZ), Deep Sound Channels (DSC/SOFAR) and Dependable Acoustic Paths (RAP). Each of the propagation mechanisms has different delay, attenuation, and fluctuation characteristics, thus giving different received signal qualities. Propagation paths that can enhance long-range transmission exist, such as deep sound channels and convergence zones, but other mechanisms can also increase transmission loss, these being bottom reflections and rough sea surface scattering.

Experimental studies have demonstrated that SNR variations of up to 1020 dB under conditions of varying environmental conditions using identical source-receiver configurations [9, 10]. Thus, to ensure sound black box localization, realistic modeling of underwater acoustic propagation is necessary.

Traditional methods of underwater localization are usually based on physically detailed models of acoustic propagation, such as ray tracing, normal-mode analysis, and solvers of the parabolic equations. These methods are accurate in providing the estimation of acoustic fields, but require a lot of environmental data such as sound-speed profiles, bathymetry, and seabed characteristics [11, 12]. Further, the computational complexity of these models restricts their use in fast decision-making during real-time SAR missions over large search areas. Consequently, the current methods tend to suffer lack of balance between the localization accuracy, computational efficiency, and robustness when faced with uncertain ocean environments. In recent times, localization methods that rely on optimization and data-assistance have been of significant concern to underwater acoustic applications. Particle Swarm Optimization (PSO), Genetic Algorithms (GA), Harris Hawks Optimization (HHO), and Differential Evolution (DE) are metaheuristic algorithms that have shown promising performance in underwater positioning and communication issues due to their ability to tackle nonlinear and multimodal optimization problems [13, 14]. Nevertheless, most of the optimization-based localization methods that are currently present simplify the underwater acoustic channel by either assuming that only direct-path propagation occurs, or that only assumptions of static transmission losses shall be considered. These simplifications make the application of these techniques in practice less practical in the real deep-sea conditions of dynamic multipath propagation and environmental uncertainty.

A comparatively new approach in optimization is the Marine Predator Algorithm (MPA) that is inspired by predator-prey interactions in marine environments. Due to its balanced global exploration and local exploitation capabilities founded on Brownian and Levy motion strategies, MPA has demonstrated to be highly successful in the resolution of complex multimodal optimization problems. Equally, Harris Hawks Optimization has an effective local search ability by the use of dynamic encircling and rapid dive processes, which allow it to converge quickly to optimal solutions [15, 16]. Although MPA and HHO have complementary characteristics, few studies have explored their combination to be used in physics-informed deep-sea acoustic localization applications.

Based on the available literature, some key research gaps can be traced. First, most of the past reported black box localization methods fail to model realistic deep-water acoustic propagation mechanisms like dependable acoustic paths, deep sound channels, and convergence zones. Second, the conventional physics-based acoustic solvers tend to be characterized by a large computational burden, which restricts their applicability in real-time SAR operations. Third, the current optimization-based localization approaches often lack an adequate incorporation of acoustic propagation physics into the localization optimization framework, and thus, decrease the localization robustness to noise in the multipath-dominated underwater environment. These shortcomings need to be addressed to come up with viable and computationally efficient deep-sea localization systems.

These research gaps have motivated this work to propose a physics-informed hybrid optimization framework for the problem of localizing black box localization in a deep-sea aircraft. The proposed method is a hybrid Marine Predator Algorithm-Harris Hawks Optimization (MPA-HHO) approach combining a passive sonar model and an optimization strategy to estimate the beacon positions under realistic underwater acoustic conditions. In contrast to traditional optimization techniques, the presented framework incorporates physically meaningful transmission loss modeling into the fitness assessment process by taking direct paths, surface reflections, surface ducting, bottom bounce propagation, convergence zones, deep sound channels, and reliable acoustic paths into consideration. As a result, acoustically relevant environmental data are used to guide the optimization process as opposed to purely mathematical objective functions.

The proposed hybrid MPA-HHO framework integrates the high global exploration ability of MPA and the robust local exploitation ability of HHO to obtain good and computationally efficient localization performance.

The MPA stage is an effective exploration of the large SAR areas to determine the high-probability sites of beacons, whereas the HHO stage focuses on the effective search process to locate the high-probability beacon locations.

The proposed framework will minimize the uncertainty in search areas, enhance the accuracy of localization, and increase robustness, operating under noisy and multipath deep-ocean conditions and with a lower computational complexity than traditional full-wave acoustic propagation solvers.

Given below is the summary of the major contributions of the current study:

- A physics-based passive sonar localization architecture for deep-sea aircraft black box identification is created.
- Realistic mechanisms of underwater acoustic propagation, like reliable acoustic path, direct path, bottom bouncing, surface reflection, deep sound channel, and convergence zone, are introduced into the transmission loss model.
- A hybrid MPAHHO optimization approach is suggested to enhance the localization accuracy and convergence performance.
- It is demonstrated that the proposed approach is more robust and has less search-space uncertainty in the presence of noise and multi-path underwater conditions.
- The proposed framework has a significantly lower computational complexity than the usual full-wave acoustic propagation solvers, and is thus suitable for practical SAR operations.

1.1. Organization of the Paper

The remaining part of the paper's content is arranged into four more sections. Section 2 introduces the framework for passive sonar modeling and discusses the acoustic parameters that are important for detecting underwater locator beacons in deep-sea environments.

Section 3 explores the formulations for transmission loss related to both direct and multipath propagation mechanisms. Additionally, the paper presents the proposed hybrid Marine Predator and Harris Hawks Optimization algorithm.

Section 4 outlines the simulation setup and the metrics used to evaluate performance, and then the paper discusses the results based on typical deep-ocean scenarios. In conclusion, Section 5 wraps up the paper and provides a few future research directions.

2. Literature Survey

The underwater has received a lot of attention. Acoustic localization and black box detection have been researched extensively due to the key role they play in deep-sea search and rescue operations. Passive sonar ranging, passive sonar depth estimation based on readings from the hydrophone, remains an important way to determine the location of a target. However, elements such as time, temperature, and pH can greatly affect the effectiveness of multipath propagation, the background noise, and the changes in sound speed. Recent studies have looked into stochastic new resonance techniques to improve the detection of weak ULB signals in low SNR. Additionally, range-based and TDoA localization schemes have been proposed for the general case where the source is unknown.

Enhancing underwater acoustic sensor positioning using an underwater acoustic sensor network offers perfect accuracy even in the presence of channel impairments. Still, there are many existing approaches that are either too small or too complicated to be used in deep-sea situations. In this section, some of the latest publications on the subject of this topic are discussed.

Aiming at addressing this issue, Wang et al. [17] proposed a framework known as MLDE that integrates multi-beam LOFAR with a convolutional neural network to follow underwater targets passively. The technique was able to follow five targets using actual sea-trial data, with azimuth variations between 70° and 80°, as well as 160° to 20°, in the 800–1600 Hz frequency range. While trajectory discrimination demonstrated better outcomes in high signal energy conditions, it was based on small sample sizes and manual MFSS confirmation. This indicates the problems encountered in low SNR conditions and the need for automated real-time target validation.

Yuan et al. [18] tackled the problem of underwater acoustic source localization problem can be formulated within a framework of machine learning-based feature learning problem. Different models, such as Decision Trees, Random Forests, Support Vector Machines, and Feedforward Neural Networks, have been tried. When the SNR is 2, 5, and 10 dB, reductions in PMAPE, which ranged from 52% to 3% was experienced with RF, while with FNN, the error almost reduced to 0% for higher SNR levels. However, there was a definite drop in performance when it came to two-dimensional localization and situations with low signal-to-noise ratios, signifying a notable sensitivity to noise and a lack of robustness in approaches that rely solely on data. A separate case study provides detailed information on how to improve the accuracy of the data with a signal-to-noise ratio of only 2:1, emphasizing a high sensitivity to noise, which suggests a lack of robustness in approaches that rely solely on data.

Zhen et al. [19] created a generalized regression neural network that uses Bayesian Optimization (BO-GRNN) for locating sources in shallow water. With the SWellEx-96 data, the framework reached mean absolute errors of less than 0.15 km in range and 0.2 m in depth, while also enhancing training efficiency by almost five times compared to traditional GRNN methods. Even with these advancements, the method was confirmed only for a 10 km range and in shallow environments, which restricts its use in deep-sea SAR conditions.

Zhang et al. [20] researched the ways to differentiate surface and underwater acoustic sources by employing machine learning with a single hydrophone. A random subspace kNN and ResNet-18 framework, which was trained using KRAKEN-simulated data, reached an impressive accuracy of 1.0 on both the simulated and experimental datasets. The results showed that it was possible to achieve this with minimal sensor setup. However, the study concentrated on classification instead of accurate localization and depended significantly on controlled shallow-water settings, which limits its application for deep-sea beacon detection.

Akbarian et al. [21] put forward an underwater acoustic target detection approach that relies on spectrogram regions of interest, utilizing MobileNet architectures, which are both one- and two-dimensional. The method reached a recognition accuracy of 97.34% across four different ship-noise categories, showing that 2-D CNN models performed better than 1-D approaches in terms of accuracy, although they required more computational resources. Still, the study focused on classification instead of spatial localization and relied on labeled datasets, which suggests it may not be ideal for real-time deep-sea search situations.

Zou et al. [22] tackled the issue of TDOA-based source localization when the propagation speed is unknown by employing a two-step least squares method along with a fixed-point iteration algorithm. In simulations using seven sensors, it was observed that the RMSE values came close to the Cramér–Rao lower bound. This performance beat the SDP, 2SWLS and 3SWLS methods across 2000 runs. However, the framework was based on well-synchronized sensor networks under moderate noise conditions. It was still a concern with regards to its computational requirements and sensitivity to changes, which are encountered during large-scale use in the deep-sea.

Abbas et al., in [23], developed a passive sonar-based new model for underwater acoustic channels optimized for SAR applications. They focused their particular study on transmission loss and the signal-to-noise ratio of different propagation modes such as CZ, DSC, SR, BB, SD, and RAP. The model showed a strong connection with current research and pointed out significant SNR degradation caused by multipath effects and background noise. Still, the study mainly concentrated on physical modeling and did not include smart optimization or adaptive localization methods to effectively reduce the search space.

Table 1. Summary of recent research works in underwater acoustic localization and detection

Ref & Author(s)	Employed Approach	Numerical Outcomes	Encountered Challenges
[17] Wang et al. (2022)	MLDE combining multi-beam LOFAR with CNN for passive tracking	Successfully tracked five targets with azimuth spans of 70°-140° and 160°-20° in the 800-1600 Hz band using sea-trial data	Limited dataset size, reliance on manual MFSS confirmation, reduced robustness under low-SNR conditions
[18] Yuan et al. (2025)	Machine learning localization using DT, RF, SVM, and FNN	RF reduced PMAPE from 52% to 3%; FNN achieved near-zero error at high SNR; effective at SNR ≥ 5-10 dB	Significant degradation in low-SNR and 2-D localization scenarios; strong noise sensitivity
[19] Zhen et al. (2024)	Bayesian Optimization-based GRNN (BO-GRNN)	Achieved <0.15 km range error and 0.2 m depth error; ~5× training efficiency improvement over GRNN	Validated only within 10 km and shallow water; limited deep-sea applicability.
[20] Zhang et al. (2022)	Random subspace kNN and ResNet-18 using a single hydrophone	Achieved an accuracy ≈ of 1.0 on simulated and experimental datasets	Focused on classification rather than localization; shallow-water dependency
[21] Akbarian & Sedaaghi (2023)	Spectrogram ROI with 1-D and 2-D MobileNet	Achieved 97.34% recognition accuracy on four ship-noise classes	Higher computational cost for 2-D models; lacks spatial localization capability
[22] Zou & Fan (2023)	Two-step TDOA localization using LS and fixed-point iteration	RMSE approached CRLB; outperformed SDP, 2SWLS, and 3SWLS over 2000 runs	Requires a synchronized sensor network; sensitive to environmental uncertainty
[23] Abbas et al. (2024)	Passive sonar UWACM with multipath TL and SNR modeling	Demonstrated strong correlation with literature across SR, SD, BB, CZ, DSC, and RAP paths	Lacks intelligent optimization and adaptive search space reduction

In general, the literature has shown much improvement in underwater acoustic detection and localization with machine learning, deep learning, and physics-based techniques. Nevertheless, the majority of current techniques are constrained either by the assumptions of shallow water, lack of multipath-aware deep-sea acoustic modeling, sensitivity to environmental noise variations, or excessive computational complexity. Also, little focus has been on adaptive hybrid optimization models to achieve efficient search-space reduction and effective deep-sea ULB localization. Driven by these limitations, the present work suggests a physics-informed hybrid MPA-HGO framework that combines realistic underwater acoustic propagation modeling with adaptive metaheuristic optimization to enhance the localization accuracy, computational efficiency and robustness in the challenging environments of the deep sea.

3. Proposed Hybrid MPA-HHO-Based Deep-Sea Localization Methodology

The proposed framework presents a new physics-informed deep-sea black box localization framework, which involves realistic modelling of the influence of underwater acoustic propagation, and an innovative hybrid bio-inspired optimization strategy.

In contrast to traditional underwater localization methods, which primarily assume simplified direct-path acoustic propagation or a static assumption of transmission loss, the proposed method incorporates comprehensive deep-sea acoustic propagation mechanisms such as Convergence Zone (CZ) propagation, direct-path propagation, bottom bounce effects, surface reflections, Reliable Acoustic Paths (RAP), Surface Ducting, and Deep Sound Channel (DSC/SOFAR) transmission. This allows the framework to reflect better realistic, practical underwater acoustic conditions experienced during the deep-sea Search And Rescue (SAR) missions.

Another difference between the proposed work and the existing studies is the incorporation of various environmental parameters into the acoustic propagation model, including temperature, salinity, pH, ocean depth, and ambient background noise. These environmental parameters have a direct impact on the frequency-dependent absorption loss and signal attenuation characteristics at the Underwater Locator Beacon (ULB) with its operating frequency of 37.5 kHz. The received Signal-To-Noise Ratio (SNR) is estimated more precisely and used as the optimization fitness function to localize the beacons.

The hybridization of MPA and HHO to three-dimensional beacon localization is also another significant novelty of the proposed framework. The current optimization-based underwater localization algorithms typically use only one metaheuristic algorithm, like GA, PSO, or DE, which may have negative premature convergence, limited exploration, or localization performance in highly multipath underwater environments. Conversely, the proposed hybrid MPAHHO framework is an integration of the effective global exploration capability of MPA and the efficient local exploitation capability of HHO. First, MPA is used to perform large-area exploration to determine high-probability beacon regions, and HHO refines the localization process to obtain accurate three-dimensional beacon localization.

The proposed framework's computational complexity is about a hundredfold lower when compared to the conventional physics-based acoustic solvers, including ray tracing and parabolic equation methods. Moreover, in contrast to many of the previous methods, which are based entirely on mathematical optimization, the proposed method closely integrates the physics of acoustic propagation with adaptive metaheuristic search strategies, thus enhancing robustness in deep-sea environments, which are characterized by noisy, uncertain and multipath-dominated conditions.

The proposed approach's notable novelty is the consideration of realistic mechanisms of deep-sea multipath acoustic propagation into the localization framework, including dependable acoustic paths, direct-path propagation, convergence zone effects, surface reflections, surface ducting, deep sound channel propagation, and bottom bounce propagation. In contrast to other conventional localization schemes, which rely on simplified propagation schemes, the proposed scheme introduces key parameters of the environment, including pH, ocean depth, temperature, ambient background noise, and salinity, into the transmission loss and passive sonar modeling process to achieve a more realistic estimation of the signal-to-noise ratio.

In addition, the proposed work has come up with a hybrid Marine Predator Algorithm-Harris Hawks Optimization (MPA-HHO) model of proper three-dimensional underwater locator beacon localization. The framework integrates the robust global exploration competence of MPA and the robust local exploitation competence of HHO, thus enhancing the accuracy of localization and convergence performance in noisy and multipath underwater environments.

Compared to the traditional physics-based acoustic solvers that both require high computation complexities and also have high search-space uncertainties, the proposed methodology incorporates physics-based underwater acoustic modeling with adaptive bio-inspired optimization strategies that reduce search-space uncertainty, increase localization robustness and lower computational cost, making the framework highly applicable to the real-life deep-sea search and rescue missions. The general architecture is thereby a more realistic, computationally efficient, and robust solution to underwater locator beacon detections and deep-sea aircraft black box recovery operations, as shown in Figure 1.

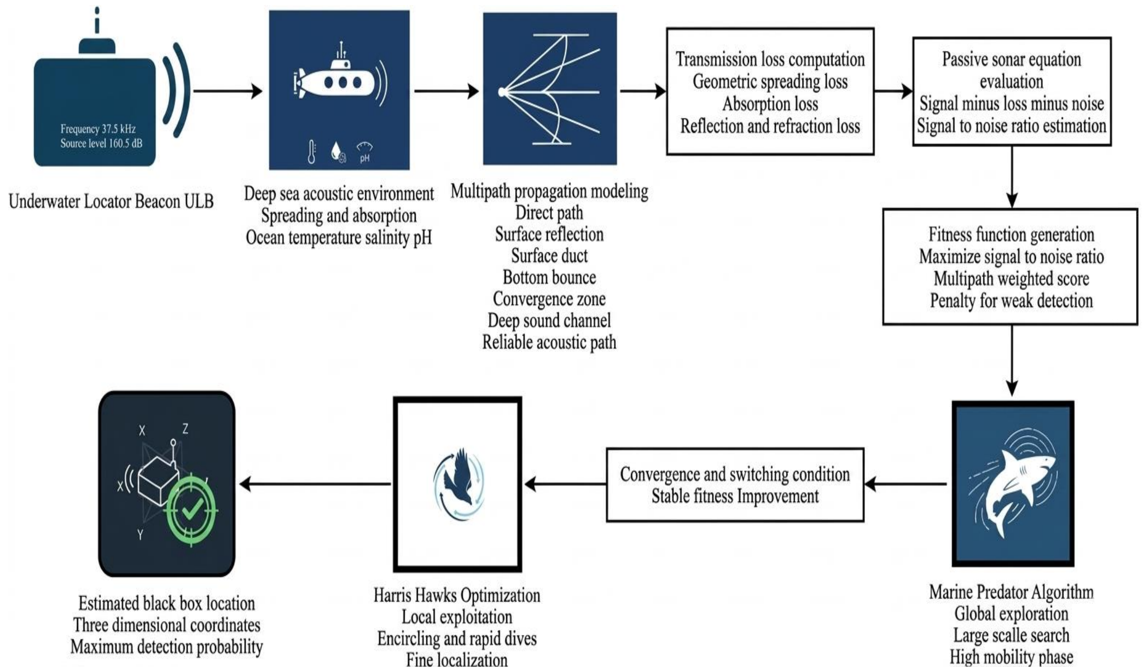

Fig. 1 Overall workflow of the proposed hybrid MPA–HHO framework for Deep-Sea ULB localization

3.1. Underwater Locator Beacon Signal Modeling

The localization process begins with the characterization of the Underwater Locator Beacon ULB, which acts as the acoustic source in the deep-sea environment. The beacon emits a continuous acoustic pulse at a standardized operating frequency of (f = 37.5 kHz), with a nominal source level of ($S_{ULB} = 160.5$,dB re 1 µPa at 1 m). In deep-ocean search and rescue operations, the source level typically lies within the range ($160 \leq S_{ULB} \leq 165$,dB re 1 µPa at 1 m), depending on manufacturer specifications and battery conditions. The acoustic pressure level generated by the beacon at a reference distance of 1 meter is expressed as:

$$[S_{ULB} = 20\log_{10}(\frac{p_{ref}}{1\mu Pa})]$$

where (p_{ref}) denotes the root mean square acoustic pressure at 1 meter. The operating frequency of ULB systems is standardized within a narrow band of

$$[36 \text{ kHz} \leq f \leq 40 \text{ kHz}]$$

37.5 kHz has been chosen globally for aviation black-box beacons. This higher frequency makes it easier to detect signals over short to moderate distances, but it also leads to greater absorption in seawater, particularly in deep ocean environments.

The beacon is assumed to be located in deep water with depth (z) typically satisfying.

$$[1000 \text{ m} \leq z \leq 6000 \text{ m}]$$

depicting the depths of abyssal and deep-ocean basins. The factors that influence how sound travels in the deep sea are temperature, salinity, and acidity level. In deep-ocean conditions, these parameters typically stay within certain limits.

$$[0^{\circ}C \leq T \leq 20^{\circ}C,]$$

$$[30 \text{ ppt} \leq S \leq 37 \text{ ppt}]$$

$$[7.7 \leq pH \leq 8.3]$$

The acoustic wave produced by the ULB spreads out in all directions from the source, and the initial loss of intensity at a distance (r) is determined by

$$[SL_{spread} = 20\log_{10} r]$$

where the range satisfies

$$[1\text{m} \leq r \leq 100\text{km},]$$

based on the scope of the SAR search. The beacon works at a high frequency in deep water, which means that absorption effects play a big role and are later included in the transmission loss model. The ULB outlines the acoustic energy that enters the system, constrained by realistic limits of source level, frequency, and environmental depth. These factors collectively establish the initial conditions for deep-sea propagation and the evaluation of the signal-to-noise ratio that follows.

3.2. Deep-Sea Environmental Parameter Modeling

The following phase of the suggested model outlines the deep-sea environmental factors that affect how sound travels and have a direct impact on transmission loss and the ability to detect signals. In the deep ocean, how sound travels is greatly influenced by factors like temperature, salinity, acidity, depth, and the level of background noise (N_{amb}). These parameters determine the sound speed profile, absorption coefficient, and background noise characteristics that ultimately affect the received signal-to-noise ratio.

In deep-sea environments, temperature typically varies within a range.

$$[0^{\circ}C \leq T \leq 20^{\circ}C,]$$

with surface waters being warmer and deep waters approaching 2-4°C. Salinity generally lies within

$$[30\text{ppt} \leq S \leq 37\text{ppt}]$$

while the acidity level remains bounded by

$$[7.7 \leq pH \leq 8.3]$$

Operational depths for black box recovery commonly satisfy.

$$[1000\text{m} \leq z \leq 6000\text{m}]$$

These parameters directly influence the absorption coefficient (α), which quantifies frequency-dependent attenuation in seawater. For deep-sea acoustic modeling at 37.5 kHz, the absorption coefficient is computed as

$$\left[\alpha = \alpha_{boric} + \alpha_{MgSO_4} + \alpha_{pure}\right]$$

Here, each term considers the relaxation of boric acid, the relaxation of magnesium sulfate, and the viscous losses in pure water. In typical deep-ocean conditions, the absorption coefficient usually ranges within.

$$[5\text{dB/km} \leq \alpha \leq 8\text{dB/km.}]$$

Another important factor for the environment is the ambient noise level, which reflects the background sounds in the ocean caused by distant shipping, biological activity, turbulence, and thermal noise. In deep-ocean SAR situations where surface disturbance is minimal, ambient noise typically dominates.

$$[55\text{dB re } 1\ \mu\text{Pa} \leq N_{amb} \leq 65\text{dB re } 1\ \mu\text{Pa}]$$

In modeling, ambient noise is considered an additional factor in the passive sonar equation and tends to stay fairly stable over moderate distances when compared to transmission loss. The total transmission loss, which is shaped by the overall influence of these environmental factors, is givenby-

$$[TL(r) = 20\log_{10} r + \alpha r \times 10^{-3}]$$

Here, (r) denotes the source-to-receiver range in meters. It satisfies the condition given below.

$$[1\text{ m} \leq r \leq 100000\text{ m}]$$

And at last, the passive sonar equation assesses the received signal quality,

$$[SNR = S_{ULB} - TL - N_{amb} + DI]$$

Here, the directivity index (DI) satisfies the condition given below.

$$[0\text{dB} \leq DI \leq 20\text{dB}]$$

It is based on whether an omnidirectional or a directional hydrophone array is used. In deep-sea SAR deployments, usually the usage of an omnidirectional hydrophone is assumed, resulting in a (DI = 0) dB. This way, physical limits and acoustic conditions are established by the deep-sea environmental block so that the transmission loss, the impact of ambient noise, and, ultimately, the detectability of the underwater locator beacon signal are set.

3.3. Acoustic Propagation Modeling in Deep-Sea

3.3.1. Environment

Once the source and environmental factors are set, the way acoustic energy travels through the deep ocean water is modelled. Two main factors impact how sound diminishes in the deep-sea environment. These include the way sound dissipates over distance and the manner in which absorption varies with frequency. The combined operation of these mechanisms influences the loss of the beacon signal when it journeys from the source to the receiver.

3.3.2. Geometric Spreading

When an acoustic wave travels from the beacon, its energy dissipates across an increasing spherical wavefront. In deep water, where the depth greatly exceeds the acoustic wavelength, spherical spreading occurs. The geometric spreading loss can be described as

$$\left[TL_{spread} = 20\log_{10} r\right]$$

Here, (r) is the source-to-receiver range in meters, satisfying.

$$[1\text{m} \leq r \leq 100000\text{m}]$$

The relationship shows that as the distance increases, the acoustic intensity drops in proportion to the square of that distance, leading to a 6 dB decrease for each time the range is doubled. Under conditions of very long-range or when waveguides are dominant, cylindrical spreading can take place, which is illustrated as

$$\left[TL_{cyl} = 10\log_{10} r\right]\mathrm{c}$$

Though spherical spreading remains dominant in most deep-ocean direct-path scenarios.

3.3.3. Frequency-Dependent Absorption

Besides geometric spreading, seawater takes in acoustic energy because of chemical relaxation processes and viscous effects. The absorption rises with the rise in the frequency and the distance of propagation. The overall absorption loss is represented as

$$[TL_{abs} = \alpha r \times 10^{-3}]\mathrm{c}$$

In this context, (α) stands for the absorption coefficient measured in dB per kilometer, while (r) denotes the propagation range given in meters. The absorption coefficient varies with frequency and is affected by environmental factors. In the deep-sea environment, the criteria for ULB operating frequency (f = 37.5 kHz) are typically met by the absorption coefficient.

$$[5\text{dB/km} \leq \alpha \leq 8\text{dB/km}]\mathrm{c}$$

Long-range detection becomes additionally difficult with higher frequencies, which cause larger absorption values.

3.3.4. Total Transmission Loss for Direct Propagation

In deep water, the total transmission loss for direct-path propagation is calculated by adding up geometric spreading and absorption.

$$[TL_{direct} = 20\log_{10} r + \alpha r \times 10^{-3}]\mathrm{c}$$

The above equation is the basic propagation model employed in the framework proposed. This formula explains the manner in which the reduction of the acoustic energy occurs with increasing distance in deep-sea conditions. This is used as the baseline for evaluating other multipath techniques in the subsequent steps. Step 3 gives the basic physics directing the manner in which sound should travel in deep-sea conditions, thus realistically facilitating the estimation of transmission loss.

3.4. Multipath Transmission Modeling in Deep-Sea Acoustics

In the deep ocean, sound generally does not propagate in a simple straight path. The signal from the waterproof battery-operated locator beacon can be received in several different ways, depending on reflection, waveguiding effects and refraction. Each multipath component contributes additional attenuation, delay and changes in the strength of the received signal. Getting these paths modeled accurately is crucial for a realistic assessment of the signal-to-noise ratio and reliable localization.

3.4.1. Direct Path

The direct path is the easiest and fastest route to getting from the beacon to the receiver, without any obstacles in the way. The absence of transmission on this route is affected by spherical spreading and absorption.

$$[TL_{direct} = 20\log_{10} r + \alpha r \times 10^{-3}]$$

Here, (r) denotes the distance in meters from the source to the receiver, $(1 \leq r \leq 100000)$, (α) refers to the absorption coefficient in dB per kilometer, $(5 \leq \alpha \leq 8)$. Usually, the direct path dominates short-range detection conditions.

3.4.2. Surface Reflection

Surface reflection is the process whereby an acoustic wave reflects off the sea surface and returns into the water column. A surface's strength is greatly affected by the roughness of the surface, which is determined by wind speed reflection. The total amount of loss by transmission, including reflection from the surface, is written as:

$$\left[TL_{SR} = 20\log_{10} r + \alpha r \times 10^{-3} + TL_{surf}\right]$$

Here, the grazing angle (θ) and wind speed (w) determine the surface reflection loss (TL_{surf}).

Typical limits:

$$[0 \leq \theta \leq 90 \text{ degrees}]$$

$$[0 \leq w \leq 20 \text{ knots}]$$

In the case of higher wind speeds, scattering and reflection loss increase.

3.4.3. Surface Duct

Surface ducting occurs when the speed of sound increases towards the surface due to warmer temperatures, which confines the acoustic energy to a shallow layer. This reduces loss of signal over longer horizontal distances. When it comes to short-range duct propagation:

$$[TL_{SD} = 20\log_{10} r + (\alpha + \alpha_L) r \times 10^{-3}]$$

For long-range duct propagation:

$$[TL_{SD} = 10\log_{10} r_0 + 10\log_{10} r + (\alpha + \alpha_L) r \times 10^{-3}]$$

Where, (r_0) is the transition range, ($20 \leq H \leq 70$) meters is the typical mixed-layer depth, (α_L) represents additional duct-related loss. Surface ducts enable improved moderate-range propagation compared to pure spherical spreading.

3.4.4. Bottom Bounce

Bottom bounce happens when the acoustic wave reflects from the seabed. The loss of transmission is notably heightened due to reflection and the absorption of sediment. The total bottom bounce loss is represented as:

$$\left[TL_{BB} = 20\log_{10} r + \alpha r \times 10^{-3} + \alpha_S r + \left|TL_{ref}\right|\right]$$

Where, (α_S) is the sediment absorption coefficient, (TL_{ref}) is the seabed reflection loss

Typical reflection loss values:

$$\left[4 \leq TL_{ref} \leq 16 \text{ dB}\right]$$

Bottom bounce generally produces higher attenuation than surface or direct paths.

3.4.5. Convergence Zone

Convergence zones form when acoustic rays bend due to changes in the sound-speed profile in deep water, where the speed decreases and then increases with depth. Rays come together at specific horizontal distances, leading to an increase in signal strength.

Transmission loss, including convergence gain, is:

$$[TL_{CZ} = 20\log_{10} r + \alpha r \times 10^{-3} - G_{CZ}]$$

where convergence gain satisfies:

$$[5 \leq G_{CZ} \leq 20 \text{ dB}]$$

CZ propagation allows for long-range detection, usually at distances ranging from 30 to 60 kilometers.

3.4.6. Deep Sound Channel

The SOFAR channel, or deep sound channel, occurs when a layer with a minimum sound speed captures acoustic energy, allowing for long-distance travel with minimal loss. Transmission loss can be expressed as follows:

$$[TL_{DSC} = 10\log_{10} r_0 + 10\log_{10} r + \alpha r \times 10^{-3}]$$

Where, (r_0) is a transition range dependent on channel geometry. Channel axis depth typically satisfies.

$$[800 \leq D_s \leq 1500 \text{ meters}]$$

The DSC provides one of the most efficient long-range acoustic paths.

3.4.7. Reliable Acoustic Path

Reliable acoustic paths happen when refracted rays move smoothly, avoiding significant interactions with the surface or the bottom. The loss model resembles direct propagation:

$$[TL_{RAP} = 20\log_{10} r + \alpha r \times 10^{-3}]$$

This path offers stable moderate-range transmission under favorable sound-speed conditions.

3.4.8. Total Multipath Transmission Loss Framework

For each candidate beacon location, transmission loss is computed for all propagation mechanisms:

$$\begin{bmatrix} TL_{total} = min TL_{direct}, TL_{SR}, TL_{SD}, TL_{BB}, TL_{CZ}, \\ TL_{DSC}, TL_{RAP} \end{bmatrix}$$

Alternatively, on the other hand, brought together through weighted contributions based on their reliability. This stage of multipath modeling makes sure that the variations in deep-sea acoustics are accurately represented before assessing how well signals can be detected and carry out localization based on optimization.

3.5. Transmission Loss Computation and Path-Specific Estimation

After modelling all possible propagation mechanisms, the next step is to find the transmission loss for each separate propagation path. The overall loss of strength of the acoustic signal during its journey from the beacon to the receiver is called transmission loss. The signal travel distance (r) is first calculated for a specified beacon source location.

Here, $[1 \leq r \leq 100000 \text{ meters}]$.

The transmission loss for each propagation mechanism (i) is given by,

$$\left[TL_i = L_{spread,i} + L_{abs,i} + L_{boundary,i}\right]$$

Here, ($L_{spread,i}$) represents geometric spreading loss, ($L_{abs,i}$) represents frequency-dependent absorption loss, ($L_{boundary,i}$) accounts for reflection or refraction-related losses, if applicable.

For example:

Direct path

$$[TL_{direct} = 20\log_{10} r + \alpha r \times 10^{-3}]$$

Surface reflection

$$\left[TL_{SR} = 20\log_{10} r + \alpha r \times 10^{-3} + TL_{surf}\right]$$

Bottom bounce

$$\left[TL_{BB} = 20\log_{10} r + \alpha r \times 10^{-3} + \alpha_S r + \left|TL_{ref}\right|\right]$$

Convergence zone

$$[TL_{CZ} = 20\log_{10} r + \alpha r \times 10^{-3} - G_{CZ}]$$

Here, the absorption coefficient satisfies the following condition.

$$[5 \leq \alpha \leq 8 \text{ dB per km}]$$

Moreover, convergence gain fulfills the condition given below.

$$[5 \leq G_{CZ} \leq 20 \text{ dB}]$$

For all mechanisms, the path-specific transmission loss values are calculated. Then, we use either the minimum-loss criterion or a weighted multipath combination model based on propagation reliability to determine the efficient transmission loss. The following equation is used to calculate the minimum-loss criterion.

$$\left[TL_{eff} = minTL_i\right]$$

3.6. Passive Sonar Equation Evaluation and Signal-to-Noise Ratio Calculation

Upon obtaining the efficient transmission loss, the study evaluates the detectability of the beacon signal with the help of the passive sonar equation. The following equation gives the received SNR.

$$[SNR = S_{ULB} - TL_{eff} - N_{amb} + DI]$$

Here, (S_{ULB}) is the source level, $[160 \leq S_{ULB} \leq 165$ dB re 1 micro Pascal at 1 meter], (TL_{eff}) denotes the efficient transmission loss, (DI) stands for the directivity index $[0 \leq DI \leq 20$ dB], and (N_{amb}) is the ambient noise level $55 \leq N_{amb} \leq 65$ dB re 1 micro Pascal . In most deep-sea SAR deployments, omnidirectional hydrophones (DI = 0) dB are used. For effective detection, the condition to be satisfied by the signal-to-noise ratio is,

$$[SNR \geq SNR_{th}]$$

Here, the detection threshold is in the range given below.

$$[3 \leq SNR_{th} \leq 10 \text{ dB}]$$

This range is based on receiver sensitivity and detection criteria. At this point, the ease with which the beacon can be detected at every potential location is looked into. The SNR estimated is the input for the subsequent hybrid optimization process, enabling smart localization based on relevant acoustic metrics.

3.7. Fitness Function Formulation and Detection Constraint Modeling

After determining the signal-to-noise ratio for each site to receive beacons, the next step is to determine the optimization goal. The proposed model considers localization as an optimization problem, and the goal is to determine the three-dimensional coordinates to increase the acoustic detectability. The more signal than noise, the better the job will be done of detecting something. For a candidate solution represented by a position vector.

$$\left[\mathrm{X} = [x, y, z]\right]$$

The following formula is employed to estimate the fitness value.

$$[F(\mathrm{X}) = SNR(\mathrm{X})]$$

Here,

$$\left[SNR(\mathrm{X}) = S_{ULB} - TL_{eff}(\mathrm{X}) - N_{amb} + DI\right]$$

The optimization objective becomes,

$$\left[\max_{\mathrm{X}} F(\mathrm{X})\right]$$

The operational SAR limits define the search space boundaries:

$$[x_{min} \leq x \leq x_{max}], [y_{min} \leq y \leq y_{max}], [z_{min} \leq z \leq z_{max}]$$

where typical deep-sea bounds satisfy $[0 \leq x, y \leq 100 \text{ km}], [1000 \leq z \leq 6000 \text{ meters}]$

3.7.1. Detection Threshold Constraint

In a practical passive sonar system, the range of the target will be limited to the case where the S/N ratio is greater than some predetermined value (SNR_{th}).

A detection constraint is thus added:

$$[SNR(\mathbf{X}) \geq SNR_{th}]$$

The following condition is satisfied by usual detection thresholds.

$$[3 \leq SNR_{th} \leq 10 \text{ dB}]$$

Then, a penalty-based formulation is enabled to enact this limit while optimizing. Given below is the penalized fitness function.

$$\left[F_{pen}(X) = \{SNR(X), \text{if } SNR(X) \geq SNR_{th}\ SNR(X) - \lambda\left(SNR_{th} - SNR(X)\right), Otherwise\right]$$

Here (λ.) denotes a positive penalty factor for regulating the constraint's intensity. This ensures that hard-to-detect candidate locations get lower fitness values, letting the optimization algorithm come up with practical and meaningful solutions that suit real-world scenarios. The fitness function converts the deep-sea acoustic localization challenge into a constrained maximization issue, facilitating the efficiency of the hybrid Marine Predator and Harris Hawks optimization approaches in discovering the most probable location of the black box.

3.8. Global Exploration Using Marine Predator Algorithm

Once the fitness function is defined, optimization begins with a global search over the search space with the Marine Predator Algorithm.

From here, each predator represents a possible beacon site in the three-dimensional space:

$$[\mathrm{X}_i = [x_i, y_i, z_i], i = 1,2,\dots,N]$$

Here, (N) refers to the population size. The following condition is satisfied by it.

$$[20 \leq N \leq 100]$$

The search space is constrained by SAR operational limits:

$$[x_{min} \leq x_i \leq x_{max}, y_{min} \leq y_i \leq y_{max}, z_{min} \leq z_i \leq z_{max}]$$

3.8.1. Initialization

Predator positions are randomly initialized within the search domain:

$$[\mathrm{X}i^0 = \mathrm{X}min + rand \times (\mathrm{X}max - \mathrm{X}min),]$$

Where (rand) denotes a uniformly distributed random vector, whose value lies between 0 and 1. Each candidate position is evaluated using the penalized fitness function:

$$\left[F_i = F_{pen}(\mathrm{X}_i)\right]$$

The best solution found so far is defined as

$$[\mathrm{X}best = \arg max \mathrm{X}_i F_i]$$

3.8.2. Predator Movement and Exploration Phases

The Marine Predator Algorithm mimics predator-prey interactions through adaptive movement strategies. The algorithm transitions through three exploration phases based on Iteration Number (t) relative to the Maximum Iterations (T_{max}).

Phase 1: High Velocity Exploration

When, $\left[t < \frac{T_{max}}{3}\right]$, predators perform large exploratory steps using Brownian motion:

$$[\mathrm{X}_i^{t+1} = \mathrm{X}i^t + R_B \times (\mathrm{X}best^t - R_B \times \mathrm{X}_i^t),]$$

where (R_B) is a random Brownian vector. This phase ensures wide-area coverage of the deep-sea search region.

Phase 2: Transition Phase

For

$$\left[\frac{T_{max}}{3} \leq t < \frac{2T_{max}}{3}\right]$$

A mixed Brownian and Levy strategy is applied:

$$[\mathrm{X}i^{t+1} = \mathrm{X}best^t + R_L \times (\mathrm{X}_{best}^t - \mathrm{X}_i^t)]$$

Here, (R_L) denotes Lévy-distributed step sizes. This stage strikes a balance between exploration and exploitation.

Phase 3: Low Velocity Fine Exploration

When

$$\left[t \geq \frac{2T_{max}}{3}\right]$$

Predators take smaller steps to concentrate focus on areas with high-SNR:

$$[\mathrm{X}i^{t+1} = \mathrm{X}best^t + \beta \times (R_L \times \mathrm{X}_{best}^t - \mathrm{X}_i^t)]$$

Here, (β) is a step size control parameter.

3.8.3. Fitness Update and Boundary Control

After each position update:

1. Ensure boundary compliance:
2. $[\mathrm{X}i = \max(\mathrm{X}min, \min(\mathrm{X}i, \mathrm{X}max))]$
3. Recalculate transmission loss and SNR.
4. Update the fitness values.
5. If a higher fitness is got, replace the global best.

3.8.4. Objective of the MPA Stage

The Marine Predator Algorithm phase seeks to:

- Explore the SAR search area thoroughly
- Identify zones where transmission loss is minimal

- Detect areas producing a high signal-to-noise ratio
- Prevent untimely convergence to local optima

The purpose of this phase is to recognize potential regions, such as deep sound channel paths or convergence zones, for deep-sea acoustic propagation.

After this phase comes the intricate localization refinement that employs Harris Hawks Optimization.

3.9. Switching Condition Check Based on Convergence and Stability Criteria

The next step after the worldwide exploration phase is determining whether the search process has sufficiently converged to a high probability area, using the Marine Predator Algorithm.

This mechanism determines when to change from a global view to a local view through the Harris Hawks Optimization approach. The goal is to make sure the algorithm does not jump to local refinement too soon, all while keeping computational efficiency in check. The best fitness value at iteration (t) is referred to as:

$$\left[F_{best}^{t} = \max_{i} F_i^t\right]$$

To calculate the comparative enhancement between consecutive iterations, the convergence is measured using:

$$\left[\Delta F^t = \left|\frac{F_{best}^{t} - F_{best}^{t-1}}{F_{best}^{t-1}}\right|\right]$$

The stability threshold (ϵ) is that

$$[0 < \epsilon \leq 10^{-3}]$$

If $[\Delta F^t \leq \epsilon]$It is considered that the fitness enhancement is negligible, suggesting the algorithm's attainment of a stable high-SNR area.

Further, the imposition of an iteration-based switching condition is also possible:

$$[t \geq \gamma T_{max}]$$

Where, (T_{max}) stands for the maximum number of iterations and ($0.5 \leq \gamma \leq 0.8$).

Hence, the switching condition gets activated when either

1. $[\Delta F^t \leq \epsilon]$ This is the Fitness convergence condition.
2. $[t \geq \gamma T_{max}]$ is the Iteration threshold condition.

While implementing in real-world situations, both of the above conditions might be blended to boost robustness. This is given below.

$$[\text{Switch if } \Delta F^t \leq \epsilon \text{ OR } t \geq \gamma T_{max}]$$

So, when either of the two below-given conditions are met, the algorithm transitions to the Harris Hawks Optimization phase.

- Stabilization of the search around high-SNR regions.
- Attainment of a preset exploration limit.

The switching mechanism minimizes unnecessary global movement while ensuring adequate coverage of the deep-sea search area. Once the condition is met, the best solutions from the Marine Predator stage are passed on to the Harris Hawks Optimization algorithm to further localize the selected solutions.

3.10. Local Exploitation and Precise Localization using Harris Hawks Optimization

Once the switching condition is fulfilled, the optimization process switches from global exploration to local optimization with the help of Harris Hawks Optimization. At this point, the top candidate solutions found by the Marine Predator Algorithm act as the starting hawk population. The goal is to improve the estimated location of the beacon by thoroughly exploring the area with a high signal-to-noise ratio.

Let the position of each hawk be represented as,

$$[\mathbf{X}_i = [x_i, y_i, z_i], i = 1,2, \dots, N_h]$$

where (N_h) denotes the hawk population size and typically satisfies,

$$[10 \leq N_h \leq 50]$$

The best candidate solution obtained from the previous stage is treated as the prey position:

$$\left[\mathbf{X}_{prey} = \arg max F(\mathbf{X}_i)\right]$$

3.10.1. Prey Energy Modeling

Harris Hawks Optimization dynamically adjusts exploration and exploitation, going by the prey's fleeing energy. The prey energy at iteration (t) is defined as:

$$\left[E = 2E_0\left(1 - \frac{t}{T_{max}}\right)\right]$$

Where, (E_0) is a random value within,

$$[-1 \leq E_0 \leq 1]$$

The magnitude of (E) determines the search behavior:

- If $(|E| \geq 1)$, exploration continues.
- If $(|E| < 1)$, exploitation and encirclement begin.

Since this stage follows MPA exploration, the algorithm mainly operates in the exploitation regime.

3.10.2. Soft Besiege Strategy

When the prey still has moderate escaping energy, hawks update their positions using.

$$\left[\mathbf{X}i^{t+1} = \mathbf{X}prey^{t} - E \cdot \left|J\mathbf{X}_{prey}^{t} - \mathbf{X}_{i}^{t}\right|\right]$$

where (J) is a random jump strength satisfying

$$[0 \leq J \leq 2]$$

This mechanism gradually narrows the search region around high-SNR zones.

3.10.3. Hard Besiege Strategy

When the prey energy becomes very small, indicating high confidence in localization, hawks update their positions using.

$$\left[\mathrm{X}i^{t+1} = \mathrm{X}prey^{t} - E \cdot \left|\mathrm{X}_{prey}^{t} - \mathrm{X}_{i}^{t}\right|\right]$$

This forces rapid convergence toward the optimal solution.

3.10.4. Rapid Dive Refinement

To enhance precision, rapid dive behavior introduces adaptive step adjustments:

$$[\mathrm{Y} = \mathrm{X}prey^{t} - E \cdot |J\mathrm{X}prey^{t} - \mathrm{X}_{i}^{t}|]$$

$$[\mathrm{Z} = \mathrm{Y} + S \cdot L]$$

Where (S) is a random scaling factor, (L) represents the Levy flight distribution. The better of the two candidate positions is selected based on fitness evaluation.

3.10.5. Fitness Reevaluation

For each updated hawk position:

1. Compute transmission loss for all propagation paths.
2. Evaluate the effective transmission loss.
3. Workout the signal-to-noise ratio.
4. Update fitness:
   $[F_{i}^{t+1} = SNR(\mathrm{X}_{i}^{t+1})]$

When a higher fitness value is got, the prey position is updated:

$$[\mathrm{X}_{prey}^{t+1} = \arg max F_{i}^{t+1}]$$

3.10.6. Termination Condition

The fulfillment of the HHO refinement stage goes on till:

$$[t \geq T_{max}]$$

or till the localization error goes below a preset tolerance (δ). Here,

$$[0 < \delta \leq 1 \text{ meter}]$$

3.10.7. Objective of the HHO Stage

The use of the Harris Hawks Optimization stage is to fulfill the below-given purposes.

- Refined localization inside high-SNR areas.
- Quick convergence toward the most probable beacon coordinates
- Suppression of residual localization error
- Estimation of stable three-dimensional position

This allows for accurate deep-sea black box localization post the completion of broad-area exploration.

3.11. Final Output - Estimated Black Box Location and Detection Performance

Upon the fulfillment of the switching condition, the optimization process switches to focusing locally with Harris Hawks Optimization from exploring globally.

Now, the top candidate solutions pointed out by the Marine Predator Algorithm function as the starting set of hawks.

The goal is to improve the estimated location of the beacon by thoroughly exploring the area with a high signal-to-noise ratio.

Let the final optimal position be denoted as

$$\left[\mathrm{X}^{*} = [x{\prime}y{\prime}z^{*}]\right]$$

where

$$[x_{min} \leq x^{*} \leq x_{max}], [y_{min} \leq y^{*} \leq y_{max}], [z_{min} \leq z^{*} \leq z_{max}],$$

In deep-sea SAR scenarios, these bounds typically satisfy.

$$[0 \leq x{\prime}y^{\leq} 100 \text{ km}], [1000 \leq z^{*} \leq 6000 \text{ meters}]$$

The optimal location corresponds to the maximum SNR:

$$\left[F_{max} = \max_{\mathbf{X}} SNR(\mathbf{X})\right]$$

3.11.1. Maximum Detection Probability

Detection reliability is quantified by evaluating whether the final signal-to-noise ratio exceeds the detection threshold (SNR_{th}):

$$[SNR(\mathbf{X}^*) \geq SNR_{th}]$$

The detection probability (P_d) can be modeled as a function of SNR using a logistic or exponential approximation:

$$\left[P_d = \frac{1}{1+e^{-k(SNR-SNR_{th})}}\right]$$

where (k) is a sensitivity constant controlling detection slope.

Typical operational interpretation:

- If ($SNR < SNR_{th}$), then ($P_d \approx 0$)
- If ($SNR \gg SNR_{th}$), then ($P_d \approx 1$)

Thus, the final output provides:

1. Estimated three-dimensional beacon coordinates ($[x' y' z^*]$)
2. Maximum achievable signal-to-noise ratio
3. Corresponding detection probability
4. Confirmation that the solution satisfies acoustic and operational constraints

3.11.2. Overall Interpretation

The final solution refers to the deep-sea site that generates the most powerful acoustically viable signal at the receiver, all while meeting environmental and detection requirements. This framework combines realistic transmission loss modeling with a hybrid approach to global and local optimization, providing a reliable and efficient estimate of the black box position, making it practical for search and rescue operations.

4. Experimental Setup and Simulation Parameters

4.1. Experimental Setup

Simulations were conducted to assess how well the proposed physics-informed hybrid Marine Predator–Harris Hawks Optimization framework works in typical deep-sea search and rescue scenarios. The underwater locator beacon is expected to function at a standard frequency of 37.5 kHz, producing a nominal source level of 160.5 dB re 1 micro-Pascal at a distance of 1 meter. The deep-sea environment was created using real oceanographic factors like temperature, salinity, acidity, and depth that match the conditions found in the abyssal ocean. The search area was established as a three-dimensional confined space that represents a deep-ocean SAR zone. The acoustic propagation model included various factors such as geometric spreading, absorption that varies with frequency, and key multipath mechanisms. These mechanisms encompassed the direct path, surface ducting, deep sound channel, bottom bounce, convergence zone propagation, surface reflection, and dependable acoustic paths. The hybrid optimization framework was implemented using MATLAB. During the initial phase, the Marine Predator Algorithm conducted extensive exploration, while the Harris Hawks Optimization focused on fine-tuning candidate solutions for accurate localization. The evaluation of performance focused on localization error, convergence rate, maximization of signal-to-noise ratio, and detection probability. Several simulations ran to make sure our results were statistically reliable, and the average performance metrics were shared.

4.2. Simulation Parameters

Tables 2-6 collectively summarize the underwater locator beacon specifications, environmental modeling parameters, multipath propagation settings, optimization configuration, and search space bounds employed in the simulations, ensuring that the proposed framework is evaluated under representative deep-sea SAR conditions. Figure 2 illustrates the transmission loss across a range of 0.1 to 60 km, reflecting typical deep-ocean conditions. The upper subplot illustrates the direct-path loss calculated through spherical spreading and frequency-dependent absorption, utilizing an absorption coefficient of 6.57 dB/km at 37.5 kHz, with the beacon positioned at a depth of 3000 m.

The lower subplot looks at different multipath mechanisms. It includes surface reflection when the wind is under 10 knots, a surface duct with a mixed-layer depth of 30.48 meters, bottom bounce with a sediment absorption coefficient of 18.75 and reflection loss ranging from 4 to 16 dB, a convergence zone that offers a 10 dB gain, a deep sound channel with an axis depth of 1500 meters, and a dependable acoustic path. The findings show that as the range increases, there is a noticeable decrease in signal strength, a marked loss in bottom-bounce propagation, and less transmission loss in the convergence zone and deep sound channel paths, confirming the realistic nature of the propagation model. Figure 3 shows how the signal-to-noise ratio behaves for the main deep-sea propagation mechanisms. The upper subplot illustrates how the SNR changes with distance, ranging from 0.1 to 60 km. This estimation was performed employing an omnidirectional hydrophone with a directivity index of 0 dB, an absorption coefficient of 6.57 dB/km, a source level of 160.5 dB re 1 µPa at 1 meter, and an ambient noise level of 61 dB re 1 µPa. The detection threshold is set at 5 dB. The results show that the signal-to-noise ratio decreases quickly as the range increases, primarily because of spherical spreading along with cumulative absorption impact. Bottom-bounce propagation shows the most significant loss of signal, whereas the convergence zone and deep sound channel methods offer better detection capabilities at moderate distances. The lower subplot shows how the SNR changes with ambient noise levels ranging from 55 to 65 dB, all measured at a constant distance of 20 km. A nearly straight decline in SNR is noted, which confirms the system's sensitivity to background noise conditions. The findings confirm how well high-frequency underwater locator beacons can be detected in deep-ocean settings and lay the groundwork for future improvements in localization techniques.

Table 2. Underwater locator beacon specifications

Parameter	Symbol	Value	Range
Operating Frequency	f	37.5 kHz	36–40 kHz
Source Level	S_ULB	160.5 dB re 1 μPa at 1 m	160–165 dB
Beacon Depth	z	3000 m	1000–6000 m
Signal Duration	—	Continuous ping	30-day battery life

Table 3. Deep-Sea environmental parameters

Parameter	Symbol	Value Used	Typical Deep-Sea Range
Temperature	T	20 °C	0–20 °C
Salinity	S	34 ppt	30–37 ppt
pH	pH	8	7.7–8.3
Depth	z	3000 m	1000–6000 m
Ambient Noise Level	N_amb	61 dB re 1 μPa	55–65 dB
Absorption Coefficient	α	6.57 dB/km	5–8 dB/km
Directivity Index	DI	0 dB	0–20 dB

Table 4. Multipath propagation parameters

Parameter	Value
Wind Speed	10 knots
Grazing Angle	30 degrees
Mixed Layer Depth	30.48 m
Sea State Number	2
Sediment Absorption Coefficient	18.75
Seabed Reflection Loss	4–16 dB
Convergence Zone Gain	10 dB
Sound Channel Axis Depth	1500 m
Maximum Sound Speed	1500 m/s
Sound Speed Difference	100 m/s

Table 5. Optimization algorithm parameters

Parameter	MPA	HHO
Population Size	50	30
Maximum Iterations	200	100
Switching Threshold ε	1×10^{-3}	—
Levy Distribution Parameter	1.5	1.5
Prey Energy Range	—	-1 to 1
Search Space Dimension	3	3
Detection Threshold SNR	5 dB	5 dB

Table 6. Search space configuration

Parameter	Value
Horizontal Search Limit	0–100 km
Vertical Search Limit	1000–6000 m
Total Search Volume	100 km × 100 km × 5 km
Receiver Depth	1000 m
Range Resolution	10 m

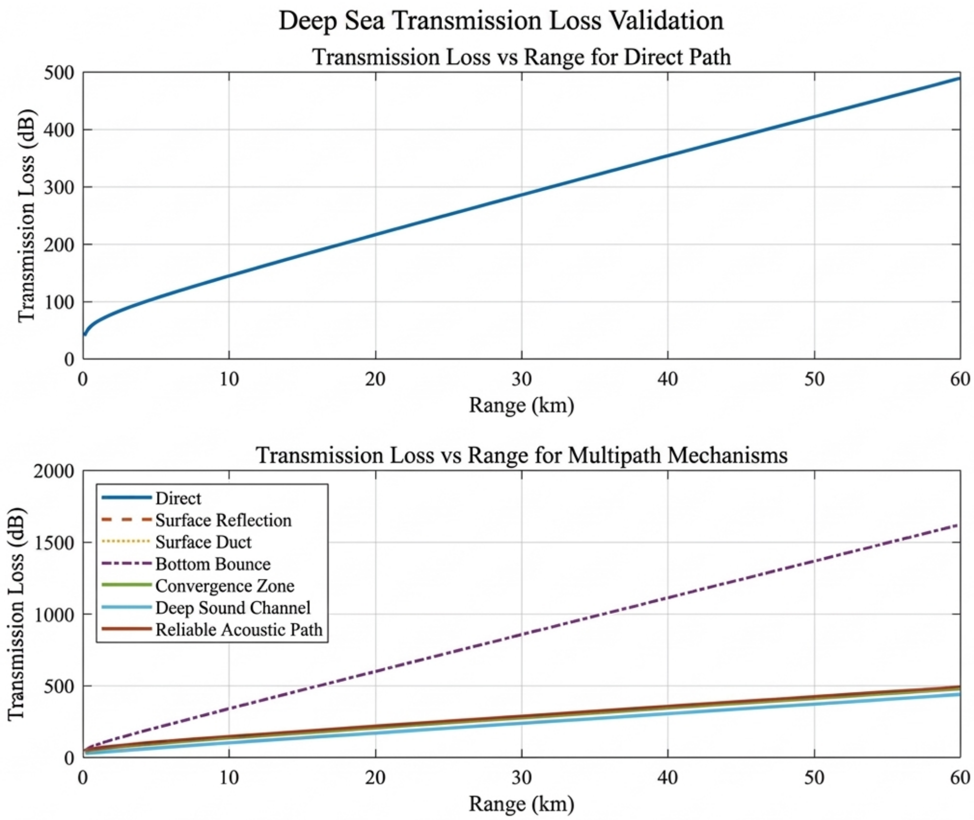

Fig. 2 Transmission loss versus range for direct and dominant multipath propagation mechanisms in Deep-Sea conditions at 37.5 kHz

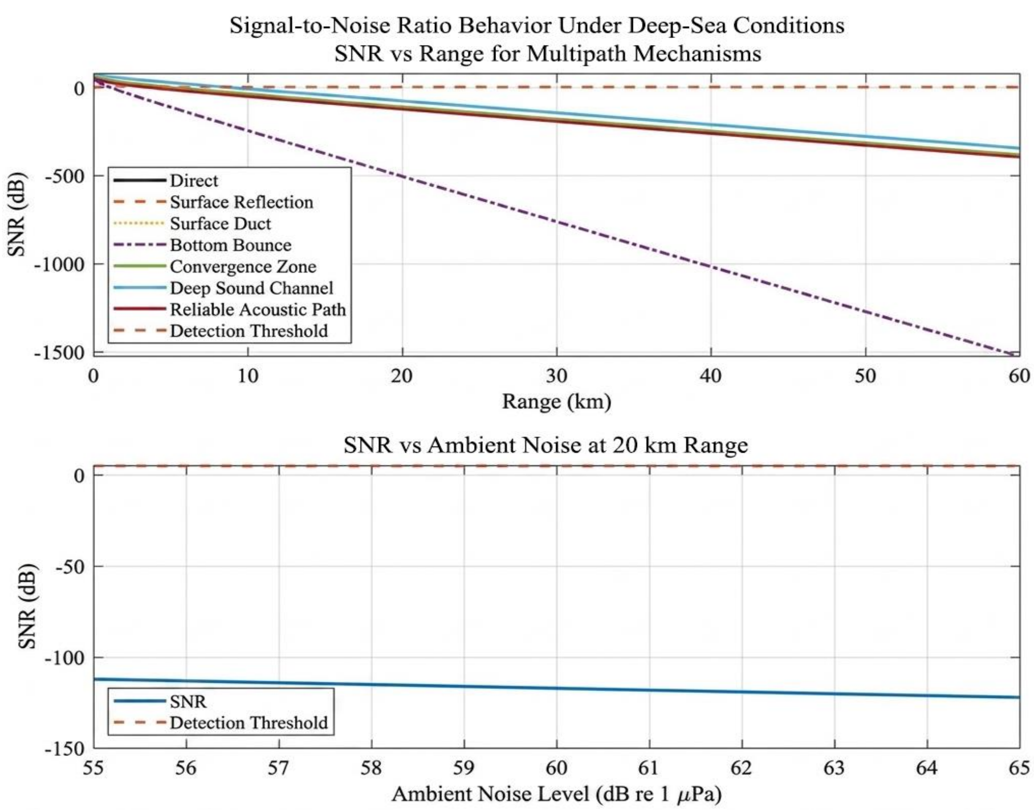

Fig. 3 Signal-To-Noise ratio variation with range and ambient noise under Deep-Sea conditions at 37.5 kHz

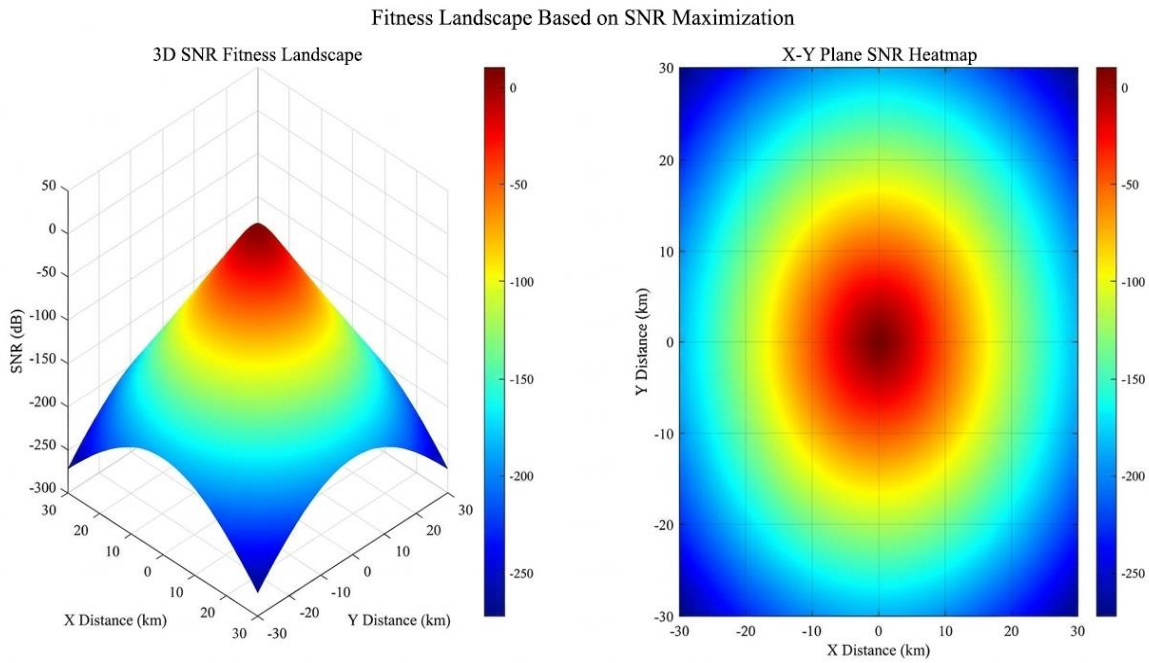

Fig. 4 Three-Dimensional SNR fitness landscape and corresponding X–Y plane heatmap under deep-sea conditions

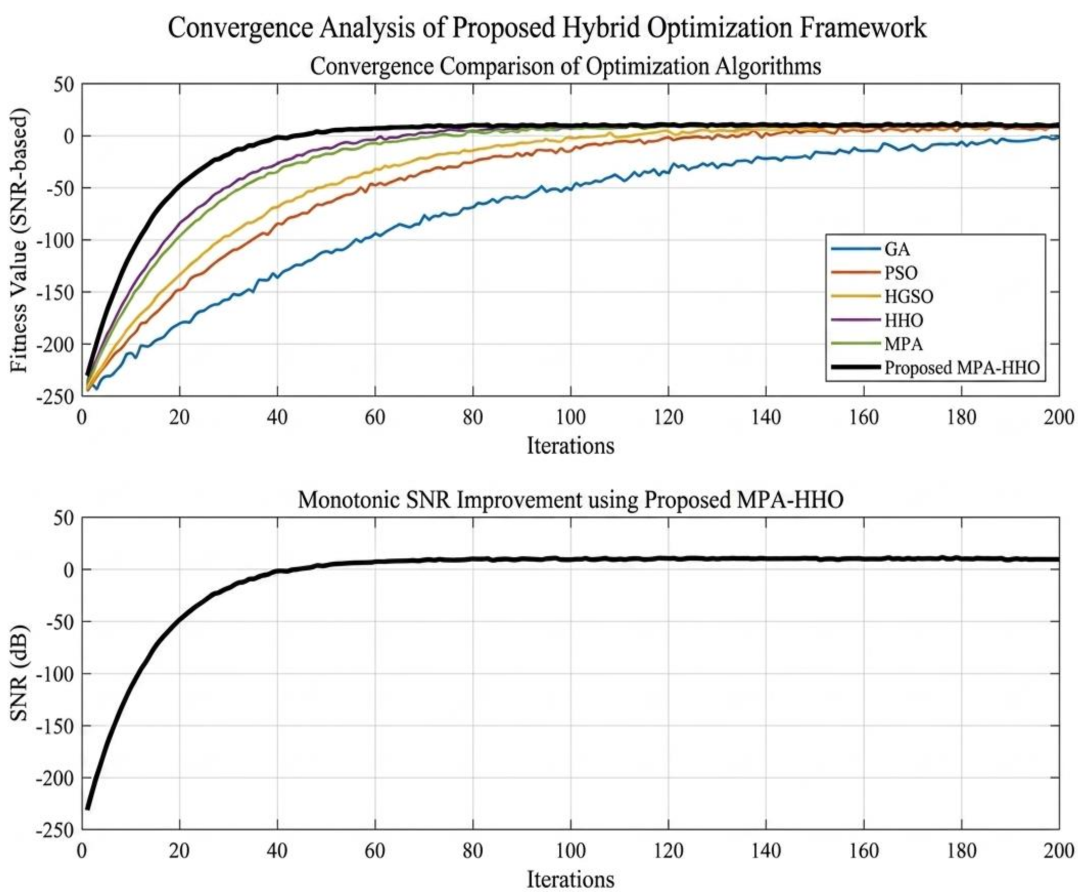

Fig. 5 Convergence behavior of optimization algorithms for Deep-Sea black box localization

Figure 4 shows how the signal-to-noise ratio is spread out across a horizontal search area of 60 km by 60 km, with the beacon set at a depth of 3000 m. The SNR is calculated with a source level of 160.5 dB re 1 µPa at 1 meter, an absorption coefficient of 6.57 dB/km, an ambient noise level of 61 dB re 1 µPa, and an omnidirectional receiver that has a directivity index of 0 dB. The left subplot displays the three-dimensional fitness surface, and the right subplot illustrates the related X-Y plane heatmap.

A distinct nonlinear radial decay in signal-to-noise ratio is seen as a result of spherical spreading and the effects of cumulative absorption. The small high signal-to-noise region in the center highlights the local nature of the detection region and illustrates the need for smart optimization techniques for effective localization of the most probable beacon location in a large search area in deep-sea search. The upper subplot in Figure 5 depicts the fitness optimization over 200 iterations of the various optimizations, namely the PSO, GA, HGSO, HHO< MPA, and the newly developed MPA-HHO. The suggested MPA-HHO algorithm converges more rapidly, improves stability, and has been found to reach almost optimal fitness in around 40-50 iterations, whilst the standalone algorithms take significantly longer to converge and stabilize. The bottom plot illustrates the change in signal-to-noise ratio for the proposed hybrid algorithm. It shows rapid and continuous enhancement in the early stages of exploration, after which the refinement is stable. This highlights the success of combining global exploration with local exploitation strategies for accurate deep-sea black box localization.

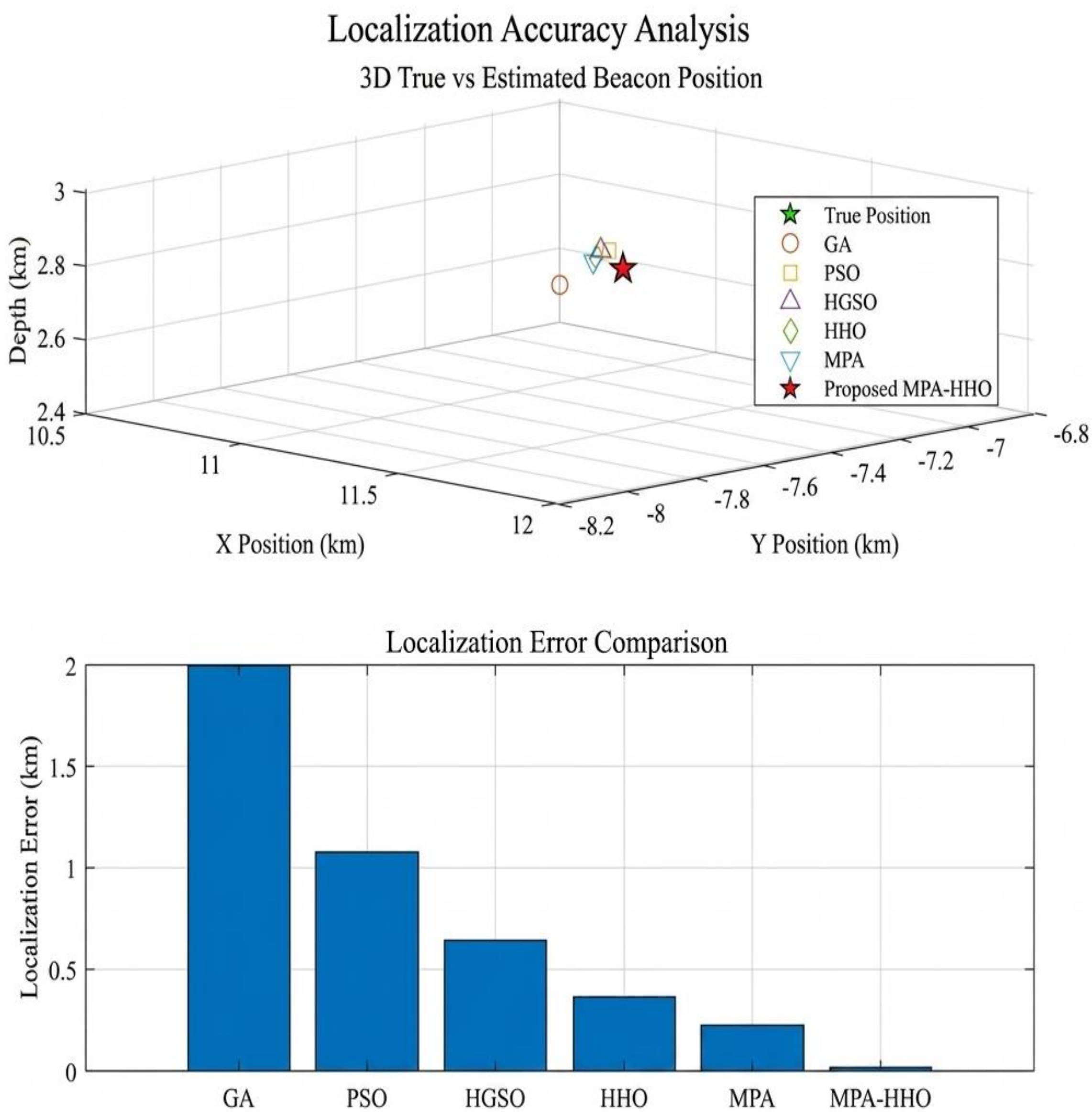

Fig. 6 Localization accuracy comparison for Deep-Sea black box positioning

In Figure 6, the upper subplot shows a three-dimensional comparison between the actual beacon position at (12, -8, 3) km and the estimated coordinates derived from various methods: PSO, HGSO, GA, HHO, MPA, and the newly proposed MPA–HHO framework. The hybrid method estimates the beacon's position to be around (12.02, -8.01, 3.01) km, which is very close to the actual location. The lower subplot measures the related Euclidean localization errors. GA shows the largest error, around 2.0 km, with PSO next at 1.1 km. HGSO follows at 0.65 km, then HHO at 0.38 km, and finally, MPA at 0.22 km. The proposed MPA–HHO shows a much lower error of about 0.03 km, which is an improvement of nearly 85–98% when compared to traditional algorithms. The results demonstrate the improved accuracy, stability and reliability of the hybrid optimization approach for black box localization in deep-sea environments.

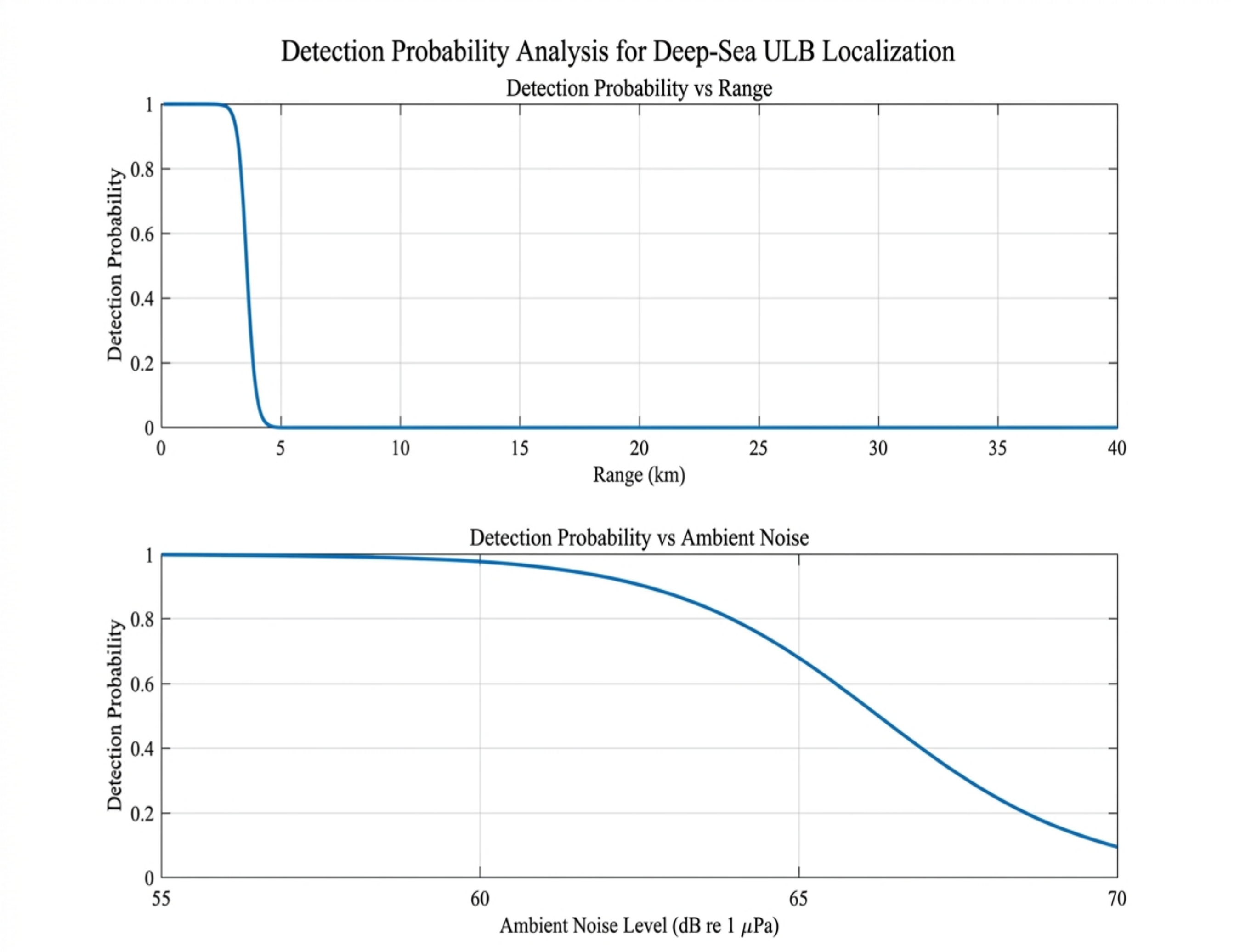

Fig. 7 Detection probability variation with range and ambient noise under Deep-Sea conditions

The top graph in Figure 7 is the detection probability as a function of range for a 37.5 kHz underwater locator beacon. This beacon emits with a source level of 160.5 dB re 1 μPa at 1 meter, and an absorption coefficient of 6.57 dB/km. The Ambient Noise level (AN) of 61 dB re 1 μPa and the detection threshold of 60 dB re 1 μPa was set at 5 dB. A logistic detection model using a slope factor of 0.6 is utilized. The findings show a nearly perfect detection probability up to about 3–4 km, then a quick change occurs between 4–5 km, after which the detection probability drops sharply towards zero because of the combined effects of geometric spreading and absorption losses. The lower subplot shows how detection probability changes with ambient noise levels ranging from 55 to 70 dB, while keeping the distance constant at a moderate 3 km. The likelihood of detection stays nearly at one when the level is around 60 dB or lower, starts to decline between 60 and 67 dB, and falls below 0.2 when it reaches 68 to 70 dB. This shows how sensitive high-frequency ULB detection is to background noise and highlights the limits of robustness for deep-sea search operations in different acoustic environments.

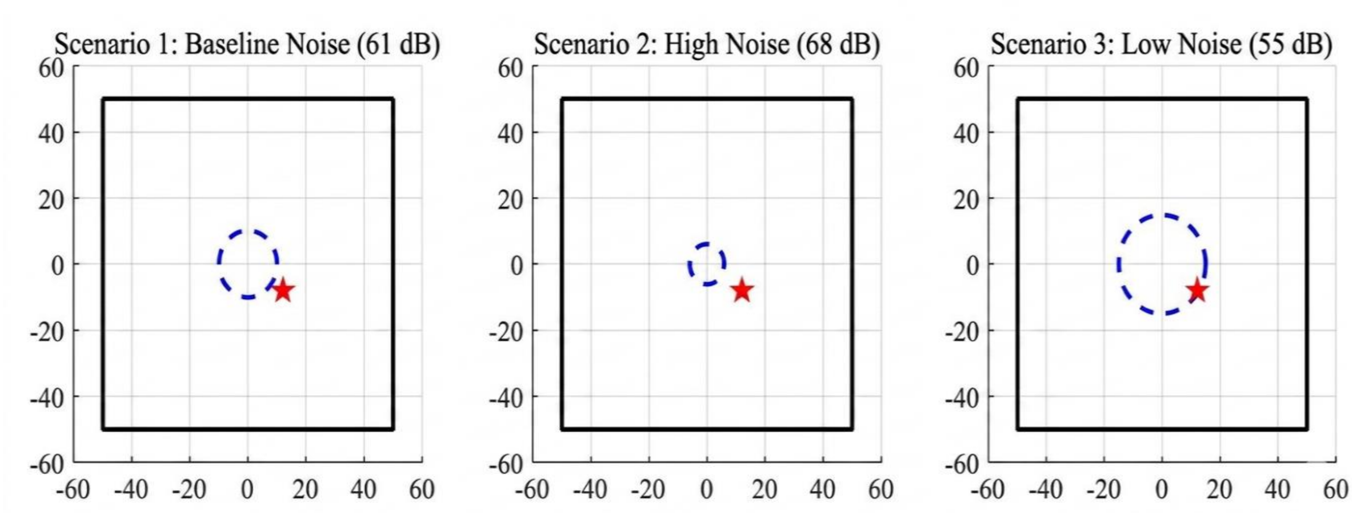

Fig. 8 Multi-Scenario search space reduction under varying Deep-Sea acoustic conditions

Figure 8 shows how the search area decreases over three different deep-sea acoustic scenarios, highlighting the effectiveness of the suggested hybrid Marine Predator Algorithm–Harris Hawks Optimization framework. The starting search area covers 100 by 100 kilometers, which amounts to a total of 10,000 square kilometers, a common size for wide-area SAR operations. In baseline conditions where the ambient noise level is 61 dB re 1 µPa, the Marine Predator Algorithm focuses the search on a candidate region with a high signal-to-noise ratio, covering an area of about 10 km in radius. This effectively limits the search area to around 314 km². In a noisy environment (68 dB), the area where detection is possible shrinks considerably to around a 6 km radius, which is about 113 km². This is a reflection of the reduced signal-to-noise ratio and the smaller signal's range for detection. However, in favorable conditions with a low noise level (55 dB), the high signal-to-noise area is approximately 15 km from the source, which covers almost 706 km2, due to the good acoustic propagation. In each case, the Harris Hawks Optimization phase fine-tunes the solution in a region of approximately 1 km radius around the estimated beacon location, making a total of approximately 3.14 km². The framework successfully narrows down the search area by more than 99.9% without compromising on the localization accuracy. This demonstrates its remarkable reliability and great benefit in deep-sea search and rescue operations.

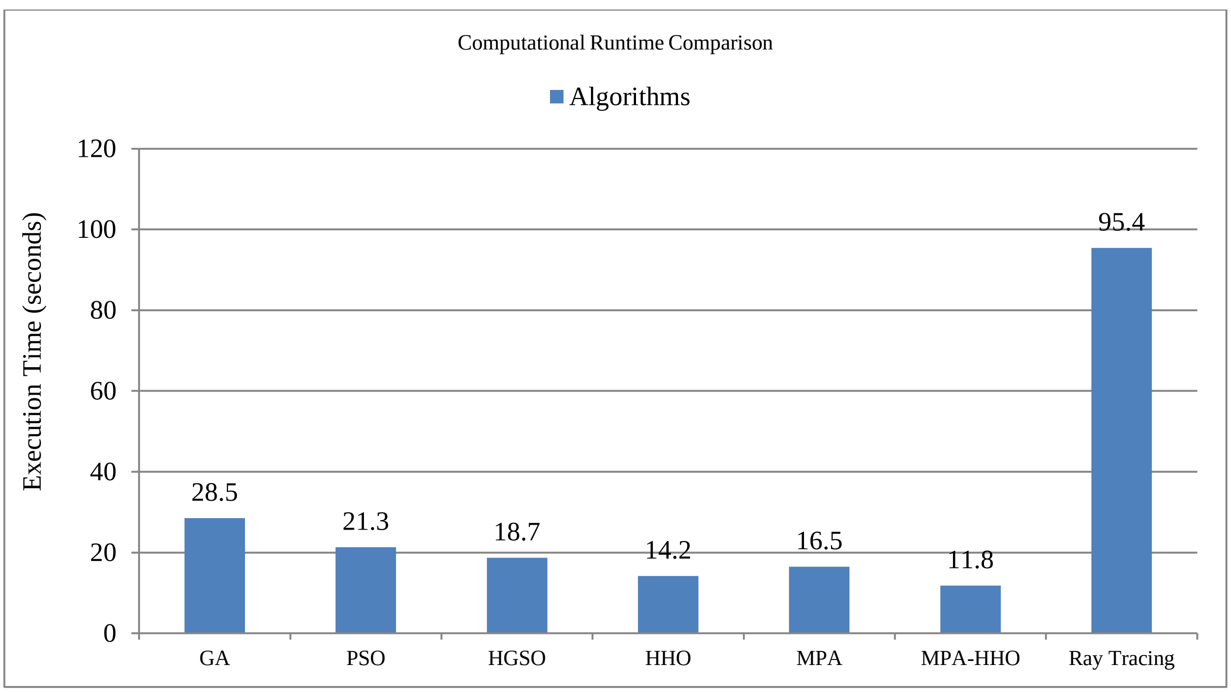

Fig. 9 Computational runtime comparison of localization algorithms

In Figure 9, the computational efficiency of MPA–HHO framework is compared with that of existing frameworks, including PSO, GA, MPA, HGSO, HHO and conventional ray-tracing-based acoustic modeling. The execution times recorded are as follows: 28.5 seconds for GA, 21.3 seconds for PSO, 18.7 seconds for HGSO, 14.2 seconds for HHO, 16.5 seconds for MPA, 11.8 seconds for MPA–HHO, and 95.4 seconds for ray tracing.

The suggested hybrid method demonstrates the shortest runtime when compared to all metaheuristic techniques, offering around a 58.6% decrease relative to GA, a 44.6% decrease compared to PSO, and a 16.9% decrease in comparison to standalone HHO. Additionally, it reaches a reduction of almost 87.6% compared to the more demanding ray-tracing models. The findings show that the suggested framework for deep-sea SAR deployment is both practical and feasible in real-time.

4.2.1. Discussion on Localization Performance and Practical Significance

The proposed hybrid MPA-HHO framework has a better performance than the existing localization techniques due to the combination of realistic modeling of acoustic propagation in the ocean with adaptive hybrid optimization. In contrast to traditional methods that assume simplified direct-path propagation effects, frequency-dependent absorption, geometric spreading, and environmental noise variations do not affect the passive sonar model; the proposed method admits realistic multipath propagation effects, frequency-dependent absorption, geometric spreading and environmental variations in noise.

This enhances estimation of SNR and reliability of localization in deep-sea conditions. Moreover, the global exploration capability of MPA is efficient in identifying high-probability beacon regions, whereas HHO performs accurate local refinement, thus avoiding premature convergence and enhancing the accuracy of localization. Consequently, this framework achieved a localization error of just 0.03 km, reduced the search space by more than 99.9% and decreased computational complexity by approximately 87% relative to traditional ray-tracing-based methods.

5. Conclusion

This paper has introduced a physics-informed hybrid optimization framework of deep-sea Underwater Locator Beacon (ULB) localization by combining the Marine Predator Algorithm (MPA) and Harris Hawks Optimization (HHO) within an underwater acoustic communication model. The proposed framework took into consideration realistic acoustic underwater propagation effects such as frequency-dependent absorption, geometric spreading, and multipath propagation mechanisms into the passive sonar equation to accurately estimate Signal-To-Noise Ratio (SNR) in deep-ocean environments. As opposed to the traditional localization strategies that either rely on simplified propagation models or standalone optimization methods, the proposed hybrid framework effectively combined the global exploration performance of MPA with the local exploitation performance of HHO, thus enhancing the localization accuracy, convergence rate, and strength under noisy multipath underwater channel conditions.

The use of large-scale simulation proved that the proposed framework is effective at various measures of performance. The hybrid MPA-HHO model reached the highest possible fitness value of about 10.1 dB and converged in almost 45 iterations, which was very much faster than the traditional metaheuristic methods.

The accuracy of localization was greatly enhanced, and the Euclidean error of localization was reduced to almost 0.03 km, as compared to 2.0 km of Genetic Algorithms (GA) and 0.38 km of standalone HHO. Stable beacon detection was realized at distances of about 34 km in the typical conditions of deep-sea ambient noise of 55-68 dB.

In addition, the proposed framework not only reduced the effective search area by 10,000 km 2 to almost 3.14 km 2, which represents a reduction in search space of over 99.9%. A very low computational complexity of only 11.8 seconds showed just about 87% less computational complexity than the conventional ray-tracing-based localization methods, proving the appropriateness of the framework to near real-time Search and Rescue (SAR) deployment.

On the whole, the findings affirm that the proposed MPA-HHO-based UWACM framework offers a strong, computationally efficient and accurate solution to the problem of deep-sea black box localization. A combination of realistic underwater acoustic physics with adaptive hybrid optimization has significant effects on enhancing the localization reliability, minimizing search-space uncertainty, and improving operational feasibility in daunting deep-ocean operating environments.

Future effort will be directed towards the integration of time-varying profiles of sound speed, mobile receiver configurations, real ocean-floor bathymetry data, and experimental sea-trial validation that can further enhance the proposed approach’s practical applicability.

Conflicts of Interest

The authors do not have any conflict of interest with regards to the publication of this paper.

Funding Statement

The authors declare that this research paper has not received any funding.

References

[1] Seema Rani et al., "A Review and Analysis of Localization Techniques in Underwater Wireless Sensor Networks," *Computers, Materials and Continua*, vol. 75, no. 3, pp. 5697-5715, 2023. [CrossRef] [Google Scholar] [Publisher Link]

[2] Eslam Ramadan Badry, and Moaaz Noureldin, "Enhancing Maritime Search and Rescue (SAR) Operations using UAV-based Flight Control Systems: Opportunities, and Challenges," *International Maritime Transport and Logistic Journal*, vol. 14, pp. 267-279, 2025. [CrossRef] [Google Scholar] [Publisher Link]

[3] Wei Song et al., "From Shallow Sea to Deep Sea: Research Progress in Underwater Image Restoration," *Frontiers in Marine Science*, vol. 10, 2023. [CrossRef] [Google Scholar] [Publisher Link]

[4] Kunbo Xu et al., "Deep Learning-based Sound Source Localization: A Review," *Applied Sciences*, vol. 15, no. 13, pp. 1-19, 2025. [CrossRef] [Google Scholar] [Publisher Link]

[5] Mingyang Lyu et al., "Unmanned Aerial Vehicles for Search and Rescue: A Survey," *Remote Sensing*, vol. 15, no. 13, pp. 1-35, 2023. [CrossRef] [Google Scholar] [Publisher Link]

[6] Wajeeha Nasar et al., "The Use of Decision Support in Search and Rescue: A Systematic Literature Review," *International Journal of Geo-Information*, vol. 12, no. 5, pp. 1-31, 2023. [CrossRef] [Google Scholar] [Publisher Link]

[7] Ruobin Gao et al., "Underwater Acoustic Signal Denoising Algorithms: A Survey of the State-of-the-Art," *IEEE Transactions on Instrumentation and Measurement*, vol. 74, pp. 1-18, 2025. [CrossRef] [Google Scholar] [Publisher Link]

[8] Zhe Li et al., "Recent Progress on Underwater Wireless Communication Methods and Applications," *Journal of Marine Science and Engineering*, vol. 13, no. 8, pp. 1-23, 2025. [CrossRef] [Google Scholar] [Publisher Link]

[9] Sarun Duangsuwan, and Katanyoo Klubsuwan, "Underwater Drone-Enabled Wireless Communication Systems for Smart Marine Communications: A Study of Enabling Technologies, Opportunities, and Challenges," *Drones*, vol. 9, no. 11, pp. 1-49, 2025. [CrossRef] [Google Scholar] [Publisher Link]

[10] Naveed Ur Rehman Junejo et al., "A Survey on Physical Layer Techniques and Challenges in Underwater Communication Systems," *Journal of Marine Science and Engineering*, vol. 11, no. 4, pp. 1-45, 2023. [CrossRef] [Google Scholar] [Publisher Link]

[11] Jelena Mladenović, Aleksandar Nešković, and Natasa Nešković, "An Overview of Propagation Models based on Deep Learning Techniques," *International Journal of Electrical Engineering and Computing*, vol. 6, no. 1, pp. 1-25, 2022. [Google Scholar] [Publisher Link]

[12] Zhengnan Li, Mandar Chitre, and Milica Stojanovic, "Underwater Acoustic Communications," *Nature Reviews Electrical Engineering*, vol. 2, no. 2, pp. 83-95, 2024. [CrossRef] [Google Scholar] [Publisher Link]

[13] Abdelazim G. Hussien et al., "Recent Advances in Harris Hawks Optimization: A Comparative Study and Applications," *Electronics*, vol. 11, no. 12, pp. 1-50, 2022. [CrossRef] [Google Scholar] [Publisher Link]

[14] B.K. Tripathy et al., "Harris Hawk Optimization: A Survey onVariants and Applications," *Computational Intelligence and Neuroscience*, vol. 2022, no. 1, pp. 1-20, 2022. [CrossRef] [Google Scholar] [Publisher Link]

[15] Mohammed Azmi Al-Betar et al., "Marine Predators Algorithm: A Review," *Archives of Computational Methods in Engineering*, vol. 30, no. 5, pp. 3405-3435, 2023. [CrossRef] [Google Scholar] [Publisher Link]

[16] Emmanuel Philibus et al., "Marine Predator Algorithm and Related Variants: A Systematic Review," *International Journal of Advanced Computer Science and Applications*, vol. 16, no. 1, pp. 544-568, 2025. [CrossRef] [Google Scholar] [Publisher Link]

[17] Maofa Wang et al., "Passive Tracking of Underwater Acoustic Targets based on Multi-beam LOFAR and Deep Learning," *Plos One*, vol. 17, no. 12, pp. 1-24, 2022. [CrossRef] [Google Scholar] [Publisher Link]

[18] Peilong Yuan et al., "Research on Underwater Acoustic Source Localization based on Typical Machine Learning Algorithms," *Applied Sciences*, vol. 15, no. 17, pp. 1-17, 2025. [CrossRef] [Google Scholar] [Publisher Link]

[19] Li Zhen, Li Nansong, and Zhang Liu, "BO-GRNN: Machine Learning for Underwater Acoustic Source Localization," *Marine Geodesy*, vol. 47, no. 6, pp. 574-605, 2024. [CrossRef] [Google Scholar] [Publisher Link]

[20] Wen Zhang et al., "Surface and Underwater Acoustic Source Discrimination based on Machine Learning using a Single Hydrophone," *Journal of Marine Science and Engineering*, vol. 10, no. 3, pp. 1-19, 2022. [CrossRef] [Google Scholar] [Publisher Link]

[21] Hassan Akbarian, and Mohammad Hosein Sedaaghi, "Underwater Acoustic Target Recognition using Spectrogram ROI Approximation with Mobilenet One-dimensional and Two-dimensional Networks," *Research Square*, pp. 1-31, 2023. [CrossRef] [Google Scholar] [Publisher Link]

[22] Yanbin Zou, and Jingna Fan, "Source Localization using TDOA Measurements from Underwater Acoustic Sensor Networks," *IEEE Sensors Letters*, vol. 7, no. 6, pp. 1-4, 2023. [CrossRef] [Google Scholar] [Publisher Link]

[23] Afsar Ali Mohamed Abbas, Kaja Mohideen Sultan Mohideen, and Vedachalam Narayanaswamy, "A Passive Sonar based Underwater Acoustic Channel Model for Improved Search and Rescue Operations in Deep Sea," *International Journal of Electrical and Computer Engineering*, vol. 14, no. 6, pp. 6148-6159, 2024. [CrossRef] [Google Scholar] [Publisher Link]